Development 126, 4489-4498 (1999)
Printed in Great Britain © The Company of Biologists Limited 1999
DEV8608

Growth cones stall and collapse during axon outgrowth in *Caenorhabditis elegans*

Karla M. Knobel, Erik M. Jorgensen and Michael J. Bastiani*

Department of Biology, University of Utah, 257 South 1400 East, Salt Lake City, UT 84112, USA
*Author for correspondence (e-mail: bastiani@bioscience.utah.edu)

Accepted 26 July; published on WWW 27 September 1999

SUMMARY

During nervous system development, neurons form synaptic contacts with distant target cells. These connections are formed by the extension of axonal processes along predetermined pathways. Axon outgrowth is directed by growth cones located at the tips of these neuronal processes. Although the behavior of growth cones has been well-characterized in vitro, it is difficult to observe growth cones in vivo. We have observed motor neuron growth cones migrating in living *Caenorhabditis elegans* larvae using time-lapse confocal microscopy. Specifically, we observed the VD motor neurons extend axons from the ventral to dorsal nerve cord during the L2 stage. The growth cones of these neurons are round and migrate rapidly across the epidermis if they are unobstructed. When they contact axons of the lateral nerve fascicles, growth cones stall and spread out along the fascicle to form anvil-shaped structures. After pausing for a few minutes, they extend lamellipodia beyond the fascicle and resume migration toward the dorsal nerve cord. Growth cones stall again when they contact the body wall muscles. These muscles are tightly attached to the epidermis by narrowly spaced circumferential attachment structures. Stalled growth cones extend fingers dorsally between these hypodermal attachment structures. When a single finger has projected through the body wall muscle quadrant, the growth cone located on the ventral side of the muscle collapses and a new growth cone forms at the dorsal tip of the predominating finger. Thus, we observe that complete growth cone collapse occurs in vivo and not just in culture assays. In contrast to studies indicating that collapse occurs upon contact with repulsive substrata, collapse of the VD growth cones may result from an intrinsic signal that serves to maintain growth cone primacy and conserve cellular material.

Key words: Growth cone collapse, Axon guidance, Substratum, *Caenorhabditis elegans*, In vivo, Time-lapse, Confocal microscopy

INTRODUCTION

The formation of synaptic connectivity requires the coordinated extension of growth cones from the neuronal cell body to the target cell (for review see Goodman, 1996; Tessier-Lavigne and Goodman, 1996). The migration of growth cones toward a selected target depends upon the adhesiveness of the underlying substratum as well as the presence of attractive and repulsive cues in the environment. How growth cones behave in the presence of these cues has been the experimental focus of neuroscientists for decades. As a result, in vitro culture systems were developed to observe growth cones as they migrate over simple substrata and contact well-defined molecular or cellular boundaries. These studies have characterized a variety of molecules that influence growth cones either by acting as positive or negative regulators of outgrowth or as adhesion proteins. Culture systems are also excellent for observing basic growth cone behaviors, such as how growth cones respond to individual cues or simple combinations of cues. However, growth cones normally migrate through a complex molecular and cellular environment in the developing animal.

Much effort has gone into understanding how growth cones behave in vivo. However, because migrating neurons are generally found deep within the developing nervous system, methods developed for observing migrating growth cones in situ require surgical dissection (Chien et al., 1993; Halloran and Kalil, 1994; Harris et al., 1987; Sretavan and Reichardt, 1993) or injection of lipophilic dyes into intact embryos (Myers and Bastiani, 1993; O'Rourke and Fraser, 1990). Furthermore, it is difficult to observe long-range growth cone migrations or easily modify the molecular composition of the growth cone or its environment in these systems.

Here we describe a method developed to observe growth cone behavior in a living unoperated animal, the nematode *Caenorhabditis elegans*. Several unusual aspects of *C. elegans* make it a particularly useful system for these studies. First, the developmental time of birth and position of all 302 neurons is known (Sulston and Horvitz, 1977; Sulston et al., 1983). Second, the final architecture and connectivity of all these neurons is known for the adult (White et al., 1986). Third, worms are transparent, so cells can be observed using Differential Interference Contrast (DIC) or fluorescence optics. Fourth, the discovery of Green Fluorescent Protein (GFP) has facilitated the study of individual cells in living worms (Chalfie et al., 1994). Fifth, neuron-specific promoters have been

identified and can be used to express GFP in specific cells. We expressed GFP in a subset of neurons and observed their growth cone migrations using time-lapse confocal microscopy. Using this procedure, we have observed stereotypical changes in growth cone shape and behavior that correlate with the cellular environment.

One well-characterized growth cone behavior is collapse, that is, the catastrophic collapse of the growth cone cytoskeleton when it encounters a repulsive cue. A variety of molecules cause collapse in vitro (Bandltow et al., 1990, 1993; Cox et al., 1990; Davies et al., 1990; Raper and Kapfhammer, 1990; Shibata et al., 1998; Walter et al., 1987). Recent in vivo studies of collapse-inducing molecules in the netrin, semaphorin and eph receptor tyrosine kinase protein families indicate that growth cones are guided away from inappropriate tissues by these molecules (Dodd and Schuchardt, 1995; Keynes and Cook, 1995; Kolodkin, 1996; Luo and Raper, 1994; Orioli and Klein, 1997). Surprisingly, these studies have failed to demonstrate that growth cone collapse occurs at repellent boundaries in vivo. By observing migrating growth cones in living and intact *C. elegans* larvae we have confirmed that growth cones collapse in vivo. However, collapse does not result in the redirection of growth cones upon contact with a specific substratum, rather, collapse appears to be a mechanism for maintaining a single terminal growth cone.

MATERIAL AND METHODS

Strains

Caenorhabditis elegans strain EG1285: *oxIs12* [*unc-47*::GFP NTX, *lin-15(+)*] *lin-15(n765ts)*] (McIntire et al., 1997) was used to visualize migrating GABA motor neuron growth cones. The CAN cell axonal process was visualized using the strain CX2644: *kyIs5* [*ceh-23*::GFP, *lin-15(+)*]; *lin-15(n765ts)* courtesy of Jen Zallen (Forrester et al., 1998).

Larval staging

50 gravid hermaphrodites were placed on a plate and allowed to lay eggs for up to 24 hours at room temperature. All hatched animals were removed from the plate. After 30 minutes, all newly hatched larvae were moved to a plate seeded with bacteria and incubated at 20°C.

Population studies

To determine the period of VD growth cone migration, we scored individual worms in populations of staged larvae after hatching. Ten new animals from a staged larval population were mounted and anesthetized every 30 minutes beginning at 13 hours after hatching. At each time point, each individual was first scored for the occurrence of the intestinal nuclei divisions or the postdeirid cell divisions using differential interference contrast optics (DIC). Then we used fluorescence optics to score GFP expression in individual VD cell bodies and the extent of VD growth cone migration.

To anesthetize staged larvae, we placed animals on 5% agarose pads containing 10 mM NaN_3. 2 μl of S-Basal or M9 were placed on top of the larvae and allowed to evaporate for five minutes. Evaporation reduces the area in which worms are distributed on the pad. A glass coverslip was placed on top of the worms and sealed with a strip of vaseline around each side. Holes in the vaseline were left in each corner and along one side of the coverslip for oxygen exchange to occur. 4 μl of S-basal were placed under each corner of the cover slip to prevent evaporation during microscopic analysis. This method of anesthesia completely paralyzes worms by stopping all metabolic and developmental processes.

Time-lapse growth cone migration studies

For time-lapse studies, larvae isolated at hatching were allowed to develop 15 hours at 20°C. Staged larvae were mounted in a bacterial pellet centered on a 5% agarose pad. 2.5 μl of 0.2% tricaine/0.02% tetramisole in M9 were placed on the worms (McCarter et al., 1997) and allowed to evaporate for 5 to 10 minutes. Coverslips were placed on the worms, sealed with vaseline and hydrated as described. Tricaine and tetramisole immobilizes worms but does not prevent metabolic and developmental processes. Tricaine acts by blocking Na^+ and K^+ channels (Frazier and Narahashi, 1975) and tetramisole is an acetylcholine agonist (Aceves et al., 1970).

We determined if immobilization affected the timing of growth cone migration in larvae. As a control, we mounted approximately ten worms on agarose pads surrounded by excess food at 15 hours after hatching. Multiple slides were sealed, hydrated and incubated at 20°C. Every 30 minutes, a new slide was removed from the incubator and scored. The effect of incubating worms under a coverslip without food was determined by isolating staged larvae at 14:30 hours post-hatching and washing them several times in S-Basal. At 15:00 hours post-hatching, washed worms were mounted on agarose pads, sealed, hydrated and placed at 20°C. Every hour a new slide was scored until VD outgrowth was finished in all worms. Experiments to determine the effects of immobilizing agents on VD outgrowth required that staged animals were isolated and washed beginning at 14:30 post-hatching as described. 2.5 μl of 0.2% tricaine/0.02% tetramisole in M9 were placed on the worms and allowed to evaporate for 5 to 10 minutes. Slides were sealed, hydrated and incubated at 20°C. A new slide was scored every hour until outgrowth was completed.

Confocal microscopy

We used a BioRad MRC 600 laser scanning confocal microscope equipped with a 1% neutral density filter to image living growth cones. We identified candidate worms by scoring the recent division of their intestinal nuclei using DIC optics. To locate migrating growth cones, we scanned selected animals at low magnification (60×, aperture 2/3 open). Selected growth cones were centered in the field of view and the scanning box size reduced to a 256 square pixel field. We increased the image zoom from 1.0 to 3.0-3.5 (magnification 60× to 180-210×) and reduced the confocal aperture. The start and stop of the Z-series were set using the motor drive. Generally, 1 μm steps between each slow scan were used with Kalman set at 1 (each Z-series averaged 3 steps). Changes in step size were modified to correspond with the aperture setting. Z-series were taken at 2 minute intervals. Bio-rad confocal 'pic' files were converted into Quicktime® movies using the 4D-Turnaround program designed by Charles Thomas and licensed from the Integrated Microscopy Resource Center at the University of Wisconsin (http://www.bocklabs.wisc.edu/imr/home2.htm) (Thomas et al., 1996).

Dorsal body wall muscle ablations

We collected embryos (*C. elegans* strain EG1524: *oxIs12 lin-15(n765ts) oxEx66* [*myo-3::*GFP*; rol-6 (su1006)*] at the 1.5-fold stage of embryonic development and placed them on agar pads as described (Bargmann and Avery, 1995). We used a Zeiss axioskop equipped with a Photonics Micropoint Laser Ablation system. Newly differentiated dorsal body wall muscle cells were identified based on their location and expression of GFP. Dorsal body wall muscle cells on the right side of the embryo were killed with 5-10 pulses of laser delivering approximately 120 μJoules of 337 nm energy per pulse. Embryos were carefully removed from the pad, placed on seeded agar plates and allowed to develop at 20°C. Worms were scored 24 hours after ablations.

RESULTS

GFP expression in growth cones

We expressed Green Fluorescent Protein (GFP) in the GABA

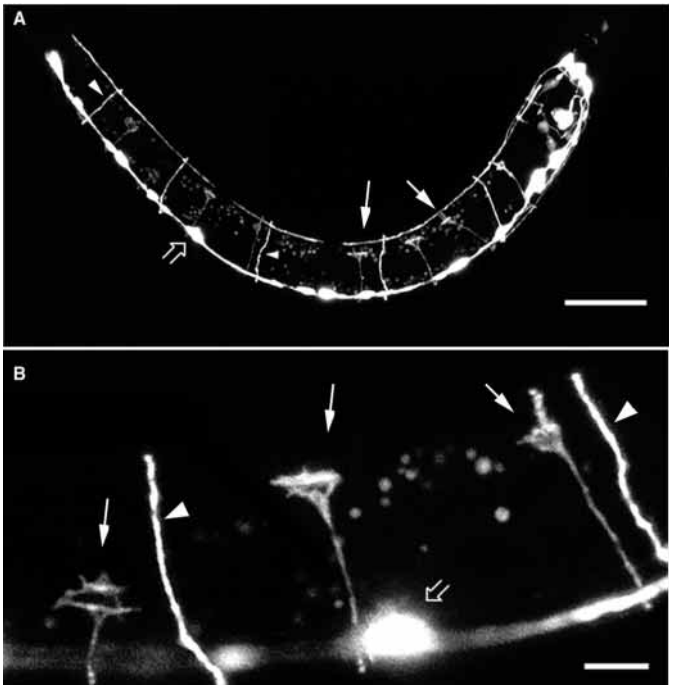

Fig. 1. VD growth cones. (A) Confocal micrograph of L2 larvae at 17 hours post-hatching. Anterior is to the right; posterior to the left. *unc-47*::GFP is expressed in the ventral nerve cord, the DD and VD cell bodies (open arrow), the DD commissures (arrowheads) and the VD growth cones (solid arrows). (B) High magnification confocal micrograph of VD growth cones in A. Filopodia extend from the round central mass of the VD10 growth cone (left arrow). The VD9 growth cone is anvil-shaped (middle arrow). The more anterior VD8 growth cone is extending a single finger toward the dorsal nerve cord (right arrow). Existing embryonic DD commissures are marked by arrowheads. Scale bar: (A) 25 μm (B) 5 μm.

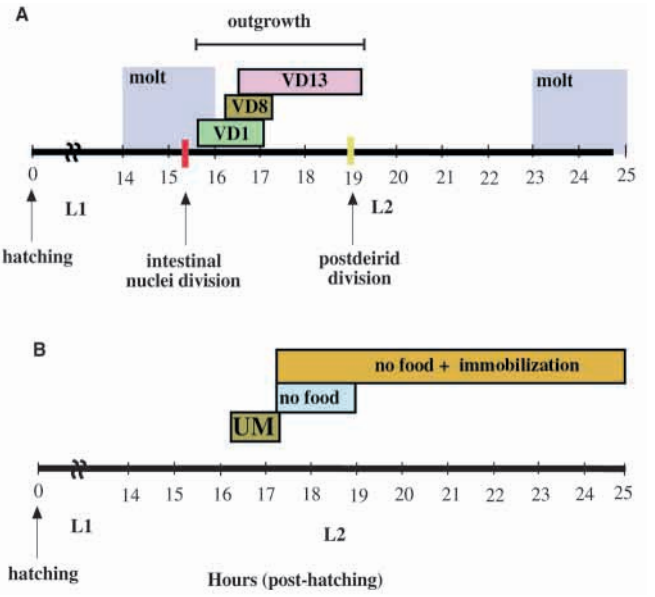

Fig. 2. Timing of VD growth cone migration. (A) Migration times for VD1, VD8 and VD13. After intestinal nuclei division occurs (15:20, red line), expression of GFP begins in the most anterior VD1 cell body (15:40). The VD1 growth cone takes 1.5 hours to migrate from the ventral nerve cord to the dorsal nerve cord (green bar). VD8 growth cone migration occurs in 1 hour (brown bar). VD13, located in the tail, takes almost 3 hours to migrate the same distance (pink bar). Division of the postdeirid neurons occurs at 19 hours (yellow line). Outgrowth of ALL VD motor neuron growth cones (from VD1 GFP expression to the completion of VD13 outgrowth) takes approximately 4 hours. (B) VD8 growth cone migration in larvae raised under normal conditions (brown bar, unmanipulated (UM)), without food (blue bar), or in tricaine and tetramisole (orange bar). In larvae raised on a plate with food, expression of GFP in VD8 begins at 16:10 and growth cone migration is done by 17:10 (brown bar, UM). In worms incubated on a microscope slide without food, VD8 cells express GFP at 17:10 and outgrowth is done by 19 hours post-hatching (blue bar**)**. Paralyzed worms express GFP at 17:10 and have completed VD8 outgrowth by 25 hours after hatching (orange bar).

neurons of the *C. elegans* nervous system using the *unc-47* promoter. *unc-47* encodes the GABA vesicular transporter and is required for transport of GABA into synaptic vesicles (McIntire et al., 1997). When GFP is expressed under the control of the *unc-47* promoter, fluorescence is observed in all mature GABA neurons, including the nineteen GABA motor neurons in the ventral nerve cord (McIntire et al., 1997). The DD and VD GABA motor neurons are generated at different times during development. The six DD motor neurons are born and differentiate during embryogenesis, when the body wall muscles are developing in the embryo (Sulston et al., 1983). Although GFP is expressed in the DD neurons at this early stage, it is not a favorable preparation for observations of growth cone migration because the animals are moving in their egg cases. The thirteen VD motor neurons are generated during the L1 larval stage (Sulston and Horvitz, 1977). At this stage, the animal can be mounted for microscopy in a fully extended posture. At the L1-L2 larval stage boundary (15-20 hours after hatching), GFP is expressed in the DD and VD cell bodies, the DD commissures and the VD growth cones (Fig. 1A). Growth cones do not express GFP as brightly as the cell bodies or DD commissures, however, they are clearly visible at the dorsal tip of extending VD axons. Most importantly, a variety of distinct growth cone shapes can be distinguished (Fig. 1B). Thus, we can observe growth cones in living animals and can characterize the behaviors that they exhibit as they migrate in vivo.

VD growth cones begin migrating during the first larval molt

Analysis of staged larvae revealed that VD outgrowth begins during the L1/L2 lethargus, a period of inactivity when the worm is molting, and ends during the middle of the L2 stage (Fig. 2A). Staged larvae were collected and allowed to develop through most of the first larval stage; after 13 hours of development, animals were mounted every 30 minutes and analyzed using DIC and fluorescence microscopy. The intestinal nuclei divide at 15 hours and 20 minutes after hatching (15:20 post-hatching), immediately before molting of the L1 larval cuticle. In the same population of animals, we scored when GFP expression began in the most anterior VD motor neuron (VD1), a VD motor neuron located midway between the head and tail of the worm (VD8) and the most posterior VD (VD13). The more anterior cells initiate GFP expression and begin outgrowth before the more posterior cells. The VD1 cell body begins expressing GFP at 15:40, the

VD8 cell body begins expressing GFP at 16:10 and VD13, the most posterior neuron, begins expressing GFP at 16:40 hours post-hatching. Outgrowth is completed when the VD13 axon reaches the dorsal cord, which occurs at about 19 hours after hatching, coincident with the generation of the postdeirid neurons. Thus, the entire process of VD outgrowth takes nearly 4 hours, beginning during the first larval molt with commencement of GFP expression in the most anterior VD1 motor neuron and ending in the second larval stage with the completion of outgrowth of VD13 (Fig. 2A).

VD growth cones migrate at slightly different rates depending upon their location along the ventral nerve cord. We could identify VD growth cones in the ventral cord soon after observing fluorescence in the cell body, so we used the initiation of GFP expression to estimate the onset of neuronal differentiation. We estimated the rate of growth cone migration by measuring the time elapsed between the start of GFP expression in an individual VD cell body and when that growth cone reached the dorsal nerve cord. VD growth cones migrate anteriorly along the ventral nerve cord approximately 15 μm before turning and extending dorsolaterally. We calculated the length of the axon trajectory by adding the distance the growth cone migrates anteriorly to half the circumference of a late stage L1 worm. We determined the diameter of these larvae by measuring the distance between the ventral and dorsal nerve cords using confocal microscopy (25 μm). Therefore the total distance VD growth cones migrate to the ventral cord is approximately 55 μm. VD1 growth cones reached the dorsal nerve cord at hour 17:10 after hatching, 1.5 hours after GFP expression began in their cell bodies at hour 15:40. VD8 growth cones reach the dorsal nerve cord 1 hour after GFP expression is observed in their cell bodies (16:10-17:10). The most-posterior neuron, VD13, migrates the same distance in approximately 2 hours and 45 minutes (16:40-19:20). Thus, the rate of VD growth cone migration in unmanipulated wild-type larvae ranges from 20 μm/hour (VD13) to 55 μm/hour (VD8).

Time-lapse analysis of growth cone migration in vivo

We observed the behavior of individual growth cones migrating in living animals using time-lapse confocal microscopy. Larvae were immobilized on agarose pads using drugs to paralyze the muscles. Confocal images of the growth cones were recorded every 2 minutes (Fig. 3, see Materials and Methods for experimental details). Fig. 3 contains a sequence of images from a single time-lapse experiment that represents all of the behaviors that we observed. All growth cones observed exhibit the same sequence of events. Moreover, we observed the same sequence of behaviors in our population studies. In our time-lapse recordings, growth cones took from 2 hours and 20 minutes to 5 hours to migrate from midway between the nerve cords to the dorsal nerve cord. Thus, the rate of migration across this distance (20 μm) ranged from 4 to 8.7 μm/hour (seven individual growth cones were analyzed), compared to 20-55 μm/hour measured in cohorts of unmanipulated well-fed animals taken from agar plates. However, retarding outgrowth during this period did not disrupt the fidelity of outgrowth. After time-lapse analysis, animals were retrieved and allowed to recover on agar plates. The structure of the nervous system and locomotory behavior of these animals was normal 48 hours after hatching.

The significantly slower rate of growth cone migration observed in our time-lapse studies occurred when worms were starved or immobilized. First, we observed that the absence of food alone affected both the timing and the rate of outgrowth. In well-fed mobile animals, VD8 began expressing GFP at 16:10 and the VD8 growth cone migration was completed in 1 hour. In the absence of food, but in conditions where animals moved freely, the initiation of VD8 growth cone migration was delayed and growth rates were slightly retarded. In these animals, the VD8 cell body began expressing GFP at 17:10 hours post-hatching and outgrowth was completed in about 2 hours (Fig. 2B). Thus, the rate of VD8 growth cone migration is almost halved in animals incubated without food during outgrowth (22.5 μm/hour). Immobilizing larvae further decreased the rate of growth cone migration. We used tricaine and tetramisole to immobilize larvae (Kirby et al., 1990). Tricaine acts by blocking Na^+ and K^+ channels (Frazier and Narahashi, 1975) and tetramisole is an acetylcholine agonist (Aceves et al., 1970). When animals were immobilized just prior to outgrowth, VD8 GFP expression began at 17:10 hours post-hatching. Outgrowth was complete in 50% of worms at 7.5 hours after GFP expression was observed in the VD8 cell body (25 hours post-hatching) (Fig. 2B). Thus, the rate of growth cone migration in immobilized animals is reduced to approximately 7.3 μm/hour. However, despite the slowed migration rates, the changes in growth cone shape and the final trajectories of the axons in immobilized larvae were identical to those observed in randomly selected unmanipulated worms. The further reduction in the rate of growth cone migration seen in the time-lapse movies (4-8.7 μm/hour) might be due to the repeated exposure of immobilized worms to the confocal laser.

Although the rate of growth cone migration is affected by the anesthetics used, the proportion of time allotted to each growth cone behavior seems to be conserved. We compared the timing of specific events observed in our time-lapse movies to the same events in unmanipulated worms. In the time-lapse movies, growth cones migrated faster along the epidermis (11 μm/hour, range 7-37 μm/hour) than through the body wall muscle (3.6 μm/hour, range 2.6-5.3 μm/hour). Similarly, in unmanipulated animals, we estimated that growth cones migrate rapidly across the epidermis (62.5 μm/hour) and slow down as they move through the muscle region (30 μm/hour; data from VD8 only). Thus, regardless of the preparation, the rate of growth cone migration on the epidermis is faster than the rate of migration along the body wall muscle. The techniques developed to observe growth cone migration in vivo slow the rate of outgrowth but do not affect the temporal dynamics of migrating growth cones.

Growth cones migrate rapidly across naked epidermis

Analysis of larvae at various time points during outgrowth revealed consistent morphological variation in the shape of growth cones (Fig. 1B). However, using static methods of analysis, it was difficult to determine if there was a stereotypical sequence of shape changes occurring during VD outgrowth. To record the behavior of individual growth cones, we generated time-lapse movies of growth cones migrating from the ventral to the dorsal nerve cord (Fig. 3). We began observing VD growth cones when they were located just ventral to the lateral nerve cord (Fig. 3, time 0:00). VD growth

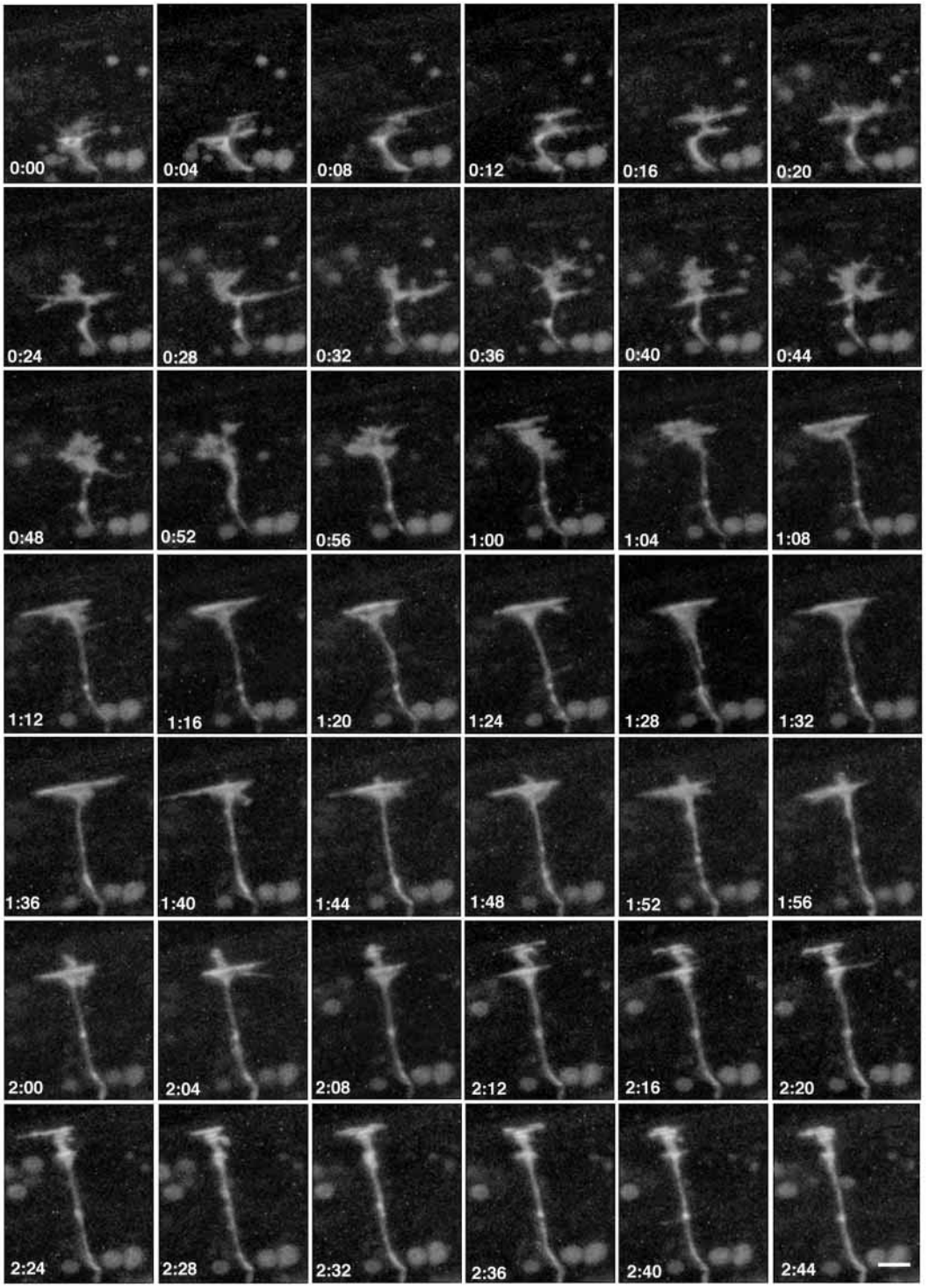

Fig. 3. Time-lapse imaging of growth cones in vivo. Growth cones were imaged every two minutes using time-lapse confocal microscopy; images taken every 4 minutes are displayed. Growth cones are migrating from the ventral nerve cord (bottom of image, not shown) to the dorsal nerve cord (cord (top of image, not shown). The round growth cone migrates dorsally until it stops, spreads out, and forms an anvil-shaped structure (0:04-0:12). This anvil-shaped growth cone extends a large lamellipodium from the leading edge of the growth cone toward the dorsal nerve cord (0:16-0:32). The growth cone retracts the lateral reaches of the anvil into its body and resumes dorsal migration until it stops and forms a second anvil located two-thirds of the way toward the dorsal nerve cord (0:36-1:00). This anvil-shaped growth cone pauses for forty minutes (1:00-1:36) before extending a finger toward the dorsal cord (1:40-1:56). As this finger approaches the dorsal side of the worm, the body of the growth cone collapses and a new growth cone forms at the tip of the finger (2:00-2:44). This growth cone continues migrating dorsally until it locates the dorsal nerve cord (not shown). Scale bar: 5 μm. [To observe the time-lapse movie from which Fig. 3 was derived, please go to the Development website: http://www.biologists.com/Development/movies/dev8608.html].

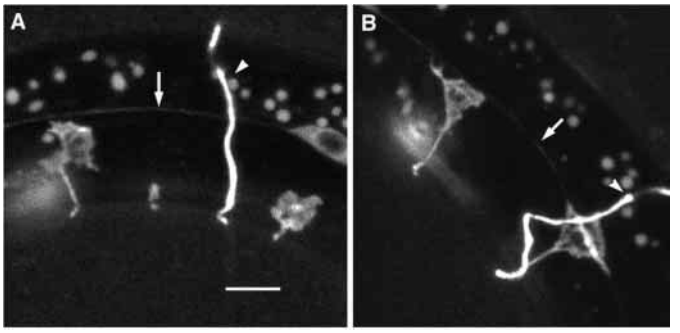

Fig. 4. Interaction of VD growth cones with the lateral CAN cell axon. (A) Confocal micrograph of rounded growth cones migrating across the epidermis. Both growth cones are spread out and round when they are ventral to the CAN cell process (arrow). Existing DD commissure is indicated by the arrowhead. (B) Confocal micrograph of growth cones contacting the lateral CAN axon. The left growth cone forms an anvil as it contacts and spreads out along the CAN process (arrow). The growth cone on the right is extending a single large lamellipodium beyond the CAN process. Scale bar: 5 μm.

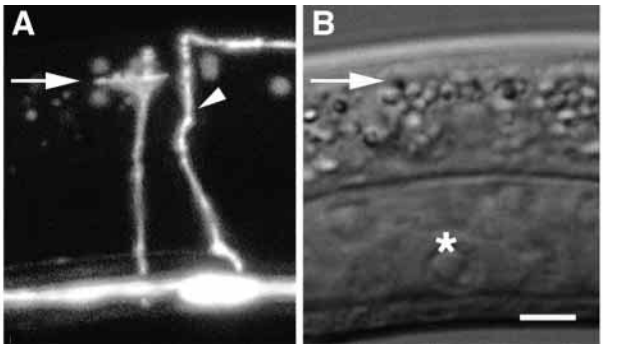

Fig. 5. VD8 growth cone forms an anvil-shaped structure at the boundary between muscle and epidermis. (A) Confocal micrograph of anvil-shaped VD growth cone. Arrow marks the leading edge of anvil. The arrowhead marks an existing DD commissure. (B) DIC image of L2 stage larvae from (A). Arrow denotes the ventral side of the dorsal body wall muscle. Asterisk marks the underlying gonad. Scale bar: 5 μm.

cones found at this location move rapidly toward the dorsal nerve cord. The central mass of rapidly migrating growth cones was generally round (Fig. 1B, left arrow) with an average width of 5.4 μm and height of 5.9 μm (*n*=3 time-lapse movies observed). As they moved dorsally, round growth cones projected filopodia up to 4 μm from the body of the growth cone (Fig. 3, time 0:36-0:56). Filopodia extended and retracted within a 2 minute period of time. These round growth cones were always observed on the lateral hypodermal (epidermal) ridge when correlated with anatomical landmarks viewed under DIC optics. In our time-lapse movies, VD growth cones migrate across the lateral epidermis at approximately 11 μm/hour (range: 7-37 μm/hour). The round shape and rapid rate of migration across the lateral epidermal cells suggests that these growth cones do not encounter many substratum boundaries or 'choice points' as they migrate across the epidermis.

Growth cones spread out along nerve fascicles

At distinct locations along their trajectory all 13 VD growth cones stopped moving, spread out and formed anvil-shaped structures (Fig. 1B: middle arrow, Fig. 3: 0:04 and 1:00). VD growth cones consistently formed anvils at the midway point between the ventral and dorsal nerve cords (Fig. 3, 0:04-0:16) roughly at the position of the lateral nerve cord. This nerve bundle is tightly associated with the underlying epidermis and consists of several axons, including the CAN neuron axonal process (White et al., 1986). To demonstrate that growth cones stop and spread out along the lateral nerve cord, we generated worms expressing GFP in the VD growth cones and the CAN cell process (Forrester et al., 1998). Growth cones were round as they approached the CAN cell process from the ventral side (Fig. 4A). Once they contacted the lateral nerve cord, growth cones spread along the process and became anvil-shaped (Fig. 4B, left). The growth cones stalled at the lateral cord for approximately 10 minutes. Although not moving dorsally, these anvil-shaped growth cones actively extend filopodia laterally and ventrally from the anvil. At their widest point, these anvils are on average 6.4 μm wide and 4.5 μm high (*n*=4). They then extended a large lamellipodia from the leading edge of the anvil toward the dorsal nerve cord and thereby crossed the lateral cord (Fig. 3, 0:16- 0:24; Fig. 4B, right). Over the next few minutes, these growth cones retracted their lateral anvil extensions, reformed their rounded shape and resumed migrating rapidly toward the dorsal cord (Fig. 3A: 0:24-0:56).

Growth cones stall at the body wall muscle

All VD growth cones form anvil-shaped structures approximately two-thirds of the way between the ventral and the dorsal nerve cords (Fig. 1; Fig. 3: 1:00-1:36). These growth cones were stalled at edge of the dorsal muscle quadrant as determined by DIC optics (Fig. 5). Anvil-shaped growth cones at the body wall muscle are on average 6.4 μm wide and 3. 8 μm tall (*n*=4). Anvil-shaped growth cones remained spread along the ventral side of the dorsal body wall muscle quadrant for up to 4 hours in our time-lapse recordings (range: 1.8 hours to 3.9 hours). For about the first half-hour filopodia extended laterally and ventrally from the leading edge of the anvil cord but no filopodia extended dorsally (Fig. 3: 1:08-1:36). Thereafter fingers of cytoplasm extended circumferentially toward the dorsal nerve cord (Fig. 1A right arrow, Fig. 3: 1:40-2:08, Fig. 6A).

It is likely that the muscle simply forms a physical barrier to growth cone migration and does not play an active role in the guidance of growth cones to the dorsal nerve cord. We laser-ablated embryonic dorsal body wall muscle cells shortly after their birth and prior to their elongation and attachment to the underlying epidermis. In experimental animals missing dorsal body wall muscle cells we observed that outgrowth was normal for the majority of axons scored after migration (88% *n*=16). Thus, these muscles were not required for guidance along this surface. In one animal we observed the growth cone in the region of laser-ablated muscle. The round morphology of this growth cone suggested that in the absence of muscle the growth cone continues rapidly migrating across epidermis unobstructed by muscle cells.

Why do anvils at the body wall muscle extend fingers, rather than lamellipodia, as observed at the lateral nerve cord? The attachment of the body wall muscles to the epidermis may present a physical barrier to the growth cone that is not present at the lateral nerve cord. Body wall muscle is attached to the

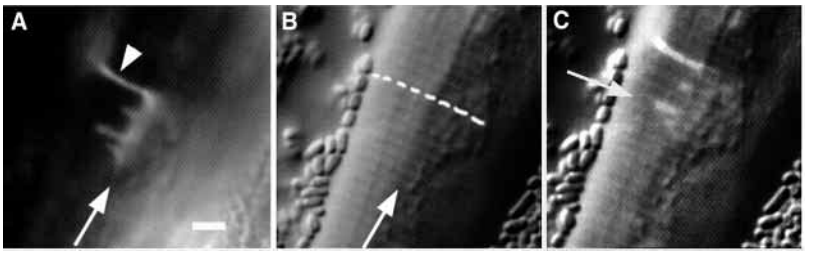

Fig. 6. Dorsal fingers align with hypodermal attachment structures. (A) Fluorescence micrograph of anvil-shaped VD growth cone extending dorsal fingers. The arrow marks the leading edge of the anvil. The arrowhead marks a DD commissure. (B) DIC image of worm in (A) focused on the cuticle and muscle. Ventral side of dorsal body wall muscle marked by arrow. Cuticular ridges (annuli) run circumferentially along the larval cuticle (dotted line) and lie directly on top of hypodermal attachment structures. (C) Fluorescent image (A) overlayed on to DIC image (B) show that growth cone fingers align with the hypodermal attachment structures (arrow). Scale bar: 5 μm.

epidermis by circumferential stripes of hypodermal attachment structures (Francis and Waterston, 1991). The stripes of hypodermal attachment structures are directly under cuticular ridges called annuli (White, 1988). The fingers projecting from the stalled growth cones aligned with the cuticular annuli as analyzed using DIC and fluoresecence microscopy (Fig. 6). Furthermore, the ridges are separated by 1 μm, which is the distance between fingers extending from the leading edge of the anvil. These data are consistent with the growth cone fingers extending between stripes of hypodermal attachment structures. These circumferential structures may thereby create narrow tunnels through which an intact growth cone cannot extend. However, the finger-like cytoplasmic extensions may be narrow enough to fit between the stripes formed by the junctions between the muscle and the epidermis.

Growth cones collapse then reform at the tips of fingers

Further migration toward the dorsal nerve cord is associated with collapse of the original growth cone and rebirth of a terminal growth cone. The anvil-shaped growth cones trapped at the ventral edge of the muscle continued to extend and retract fingers between the muscle and epidermis for greater than 1 hour. Thereafter, a single finger would predominate and extend through the body wall muscle quadrant to the dorsal side of the muscle (Figs 1B, 3). When this occurred, all secondary fingers extending from the anvil retracted and the body of the growth cone began collapsing (Fig. 3: 2:04-2:44). As the original growth cone collapsed, a new growth cone formed at the dorsal tip of the predominating finger. It took approximately 2 hours from the time that fingers began extending from the leading edge of an anvil to the time of formation of a new dorsal growth cone. While the growth cone was collapsing, we observed that fluorescent material from the ventral growth cone flowing toward the dorsal tip of the predominant finger. The new growth cone expanded and resumed migration toward the dorsal nerve cord. At the dorsal cord, the processes of the growth cone were obscured by the fluorescence of the existing nerve cord and we stopped imaging.

DISCUSSION

In this paper, we describe a method for imaging growth cones in living *C. elegans*. Specifically, we studied the outgrowth of the postembryonic VD motor neurons. The growth cones of these neurons move rapidly when they are travelling across the surface of unobstructed epidermis. VD growth cones stall for lengthy periods when they encounter novel substrata such as perpendicular nerve fascicles or groups of muscles that are tightly attached to the epidermis. Growth cones overcome these obstacles in different ways. In the case of the nerve fascicle, they extend large lamellipodia across the fascicle. At the muscle, growth cones extend narrow fingers between the muscle and the epidermis. One of these fingers eventually reaches the other side of the muscle; this finger then becomes the new terminus of the axonal process. The old growth cone collapses and a new growth cone is born at the tip of the finger (Fig. 7).

Wave of differentiation

VD motor neuron growth cone migration begins during the first larval molt and ends approximately 4 hours later during the second larval stage of development. The intestinal nuclei divide immediately before the expression of GFP in the anterior VD cell bodies begins. Interestingly, differentiation of the VD motor neurons precedes as an anterior-to-posterior wave. Previous researchers had observed that the VD cells are born in an anterior-to-posterior birth order (Sulston and Horvitz, 1977). We observed that the most anterior VD neurons express GFP serially followed by the more posterior neurons. Recently Hallam and Jin (1998) describe a similar anterior-to-posterior trend for the rewiring of the embryonic D motor neurons. Finally, axonal outgrowth from the VD neurons also proceeds as an anterior-to-posterior wave. This anteroposterior pattern of neuronal differentiation has been described in insects and

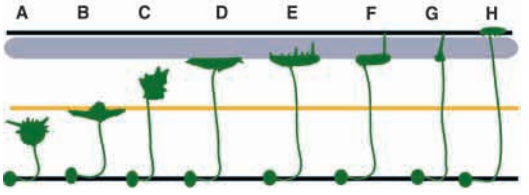

Fig. 7. Migrating VD growth cones exhibit a variety of behaviors as they contact different substrata. The X-axis represents time, the Y axis represents dorsoventral location (ventral is on the bottom, dorsal on top). (A) Rounded growth cones (green) migrate across the epidermis. (B) Growth cones form anvils at the lateral nerve cord (yellow line) then extend lamellipodia beyond the leading edge of the anvil. (C) Growth cones resume migrating across the epidermis. (D) Growth cones form anvil-shaped structures at the dorsal body wall muscle (grey). (E) Anvil-shaped growth cones extend fingers toward the dorsal nerve cord. (F) A single finger predominates and extends beyond the dorsal extent of the muscle. (G) Growth cones located on the ventral side of muscle collapse. (H) New growth cones form at the tip of the predominant finger. These new growth cones locate then bifurcate along the dorsal nerve cord (black line).

vertebrates (Hatta and Kimmel, 1993; McMahon, 1993), suggesting that there may be something fundamental about this process as an organizing factor in development of the nervous system.

Although axon outgrowth and remodeling is initiated during lethargus, the period of inactivity associated with molting, outgrowth is completed when the postdeirid neurons are generated nearly half way through the L2 larval stage. Moreover, shortly after VD growth cone migration is finished, differentiation of the VD presynaptic domains is observed in the ventral nerve cords (Hallam and Jin, 1998). This is associated with the disappearance of DD synapses in the ventral cord and the formation of DD synapses in the dorsal cord. Larvae are active during this period. It is a mystery how a larva can remain coordinated as it is remodeling its motor nervous system during this period.

Rates of growth cone migration

Our observations indicate that VD growth cones in undisturbed, well-fed, motile animals have an overall migration rate of 20-55 μm/hour depending upon the location of the neuron along the anteroposterior axis. In our movies, we observed that the rate of migration depended upon where the growth cone was with respect to the dorsoventral axis and obstacles along the substratum. How does the overall rate of *C. elegans* growth cone migration in vivo compare to those of other growth cones studied in culture and in situ? Cultured growth cones migrate on very simple, well-defined surfaces and do not encounter the normal environmental obstacles and cues found in vivo. On simple substrata like laminin, cultured growth cones migrate from 12-15 μm/hour (Bandtlow et al., 1990; Hubener et al., 1995) to 90 μm/hour (Buettner and Pittman, 1991) depending on substratum composition and the inclusion of growth-promoting molecules. In dissected embryonic preparations, growth cones can migrate from 30 μm/hour (Sretavan and Reichardt, 1993) up to 80 μm/hour (Halloran and Kalil, 1994). In intact embryos, neurons injected with lipophilic dyes migrate from 8 μm/hour (Myers and Bastiani, 1993) to 70 μm/hour (Harris et al., 1987). Thus *C. elegans* growth cones migrate at rates comparable to those observed for other species and preparations.

We observed that growth cones migrate rapidly across unobstructed epidermis, but stop at various points along their trajectory. Therefore the overall rate of migration consists of periods of motility separated by stalls. For example, VD growth cones migrate rapidly across the epidermis, but slow down as they encounter obstacles to migration. Previous observations of growth cone migration in situ indicated that migrating growth cones exhibit periods of motility and stalling (Halloran and Kalil, 1994) similar to what was observed in our own studies. However, we are able to correlate similar variations in migration rate to the contact of specific cellular substrata by the growth cone.

We also discovered that the observed rate of growth cone migration was influenced by the culture conditions and immobilizing agents that we used. For example, growth cones in unfed animals start migrating later and take longer to reach their target in the dorsal nerve cord. It is possible that the inability of these animals to eat reduces the production of metabolic energy that is available to the neurons. In addition, methods used to immobilize the worms further decreased the rate of migration. The presumed targets of these anesthetics are acetylcholine receptors (tetramisole) and potassium channels (tricaine) in the *C. elegans* body wall muscle. However, it is possible that these drugs slow growth cone migration by acting directly on the VD neurons and disrupting the physiology of the cell. Alternatively, these drugs may affect the general metabolism of the worm. For example, pharyngeal pumping is stopped in animals immobilized with tricaine and will thereby lead to starvation even in the presence of food. Of course, the most important issue is whether slowed growth cones can respond to guidance cues and eventually form a normal nervous system architecture. We found that neither the lack of food nor the treatment of animals with these paralytic agents affected the growth cone shapes or the ultimate fidelity of outgrowth compared to untreated animals.

Stalling

Growth cones move rapidly across the unobstructed epidermis, but when they contact obstacles lying perpendicular to their direction of migration, like nerve fascicles and body wall muscle, growth cones stop advancing and spread horizontally to form anvil-shaped structures. Anvil-shaped growth cones stall for varying amounts of time at different positions along their trajectory. The length of the pause depends upon the substratum encountered by the growth cone. For instance, when growth cones contact the lateral nerve process, they stall only briefly before extending lamellipodia beyond the axon, whereas they can stall at the body wall muscle for hours. Why do growth cones stall? One possibility is that the growth cone is simply unable to respond to the new substratum, such as a nerve fascicle, even though the pathway is unimpeded. Thus, stalling may represent a lag imposed by the signal transduction pathways that are required to reorganize surface molecules or the cytoskeleton. Once the correct cell adhesion molecules or growth cone specializations are in place then the growth cone can overcome the obstacle. Alternatively, these pauses could be caused by the presence of a physical barrier that blocks further migration. Specifically, reconstructions from serial electron micrographs of adults indicate that the VD growth cone passes under the lateral nerve cord, that is, the growth cone stays in contact with the surface of the epidermal cell rather than the overlying basal lamina (Durbin, 1987). The lateral nerve cord axons may still be attached to the surface of the epidermal cell from their earlier migrations and the VD growth cone is blocked by these cell-cell junctions. Eventually, the growth cone overcomes this block, perhaps by detaching the axons of the lateral cord from the substratum and proceeding underneath them. In the case of the body wall muscle, it is already known that the muscle is tightly attached to the epidermis. Here, it appears that the growth cone does not detach the muscle from the epidermis, but squeezes through the narrow channels between the attachment structures.

Collapse

Collapse of migrating growth cones has been observed in vitro in response to extrinsic collapse-inducing factors (Colamarino and Tessier-Lavigne, 1995; Meima et al., 1997; Raper and Kapfhammer, 1990; Shoji et al., 1998). However, in vivo studies implicate these factors in the steering of growth cones, not the collapse of growth cones (Kolodkin, 1996; Kolodkin et al., 1992; Matthes et al., 1995; Orioli and Klein, 1997; Shoji

et al., 1998; Taniguchi et al., 1997; Yu et al., 1998). Thus, the physiological relevance of growth cone collapse is unknown. In contrast to these previous studies, we observed that growth cone collapse occurs reproducibly in vivo. More interestingly, growth cone collapse is not associated with the redirection of axonal trajectories. Instead, collapse occurs while the axon continues extending in the same dorsal direction. After a lengthy pause at the body wall muscle, the growth cone extends cytoplasmic fingers toward the dorsal nerve cord. When a growth cone finger finally reaches the dorsal side of the muscle, the central mass of the original growth cone collapses and a new growth cone forms at the dorsal tip of the finger.

Why would growth cone collapse occur without affecting the direction of migration? In general, individual axons maintain a single growth cone at their tips. In addition to being a steering mechanism, we propose that growth cone collapse ensures that individual axons have only one functional growth cone at their tips. This implies that there is an intrinsic mechanism present within the axon and growth cone that is responsible for maintaining growth cone 'primacy', that is, that only one growth cone is found at the tip of the extending axon at any point in time. The presence of a growth cone at the ventral side of the body wall muscle and a new growth cone at the tip of the extending axon is not compatible with the growth cone's intrinsic program to maintain primacy. Growth cone collapse at the muscle may thereby prevent the unnecessary branching of growth cones.

How does the growth cone know when to collapse? We present two simple models. In the first model, collapse is not an active process, instead it is simply the passive rearrangement of the cytoplasm to another, albeit distant, site of the same growth cone. Thus, the mechanism of collapse does not require any specialized signals other than those required for normal growth cone activity. In the second model, growth cone collapse is an active response to a collapse-inducing signal encountered in the substratum environment. If the collapse-inducing signal is located along the dorsal axis of the worm, then collapse of the growth cone would be initiated by contact of the finger with the substratum.

In summary, VD growth cones in *C. elegans* migrate rapidly over unobstructed epidermis, however, physical or molecular barriers can block migration. The growth cone moves beyond these obstacles by either extending a lamellipodia that is capable of penetrating the block, or by projecting narrow cytoplasmic fingers that tunnel through openings in the barrier. Moreover, our studies suggest that growth cone collapse is an important mechanism for maintaining the morphology of migrating growth cones. Growth cone collapse appears to be initiated by intrinsic signals to maintain primacy of the terminal growth cone. In the future, these studies will allow for the identification of mutants defective in these specific behaviors and characterization of the molecules that mediate these behaviors.

We would especially like to thank John White and all members of the Integrated Microscopy Resource Center (IMR) for providing support and equipment for the time-lapse microscopy experiments. We are indebted to all members of the Jorgensen and Bastiani laboratories for their insight and support. We thank Dr Ed King for help with the confocal microscope, Drs Beverly Benson and Jean-Louis Bessereau for comments on the manuscript, Kim Schuske for *oxIs12* and Jen Zallen for *kyIs5*. We also thank Andy Fire for the *myo-3*::GFP plasmid used in the laser ablation experiments. All time-lapse microscopy experiments were performed at the IMR, University of Wisconsin, Madison, (NIH RR00570). Work was supported by an NIH Developmental Biology training grant to K. K., and NIH grants NS 34307 to E. M. J. and NS 25387 to M. J. B.

REFERENCES

Aceves, J., Erlij, D. and Martinez-Maranon, R. (1970). The mechanism of the paralysing action of tetramisole on *Ascaris* somatic muscle. *Br. J. Pharmacol.* **38**, 602-607.

Bandltow, C. E., Schmidt, M. F., Hassinger, T. D., Schwab, J. E. and Kater, S. B. (1993). Role of intracellular calcium in NI-35-evoked collapse of neuronal growth cones. *Science* **259**, 80-83.

Bandtlow, C., Zachleder, T. and Schwab, M. E. (1990). Oligodendrocytes arrest neurite growth by contact inhibition. *J. Neurosci.* **10**, 3837-3848.

Bargmann, C. I. and Avery, L. (1995). Laser killing of cells in *Caenorhabditis elegans*. In *Methods in Cell Biology*, vol. 48 (ed. H. F. Epstein and D. C. Shakes), pp. 225-250. San Diego: Academic Press.

Buettner, H. M. and Pittman, R. N. (1991). Quantitative effects of laminin concentration on neurite outgrowth in vitro. *Dev. Biol.* **145**, 266-276.

Chalfie, M., Tu, Y., Euskirchen, G., Ward, W. W. and Prasher, D. C. (1994). Green fluorescent protein as a marker for gene expression. *Science* **263**, 802-805.

Chien, C.-B., Rosenthal, D. E., Harris, W. A. and Holt, C. E. (1993). Navigational errors made by growth cones without filopodia in the embryonic *Xenopus* brain. *Neuron* **11**, 237-251.

Colamarino, S. A. and Tessier-Lavigne, M. (1995). The axonal chemoattractant netrin-1 is also a chemorepellent for trochlear motor axons. *Cell* **81**, 621-629.

Cox, E. C., Muller, B. and Bonhoeffer, F. (1990). Axonal guidance in the chick visual system: posterior tectal membranes induce collapse of growth cones from the temporal retina. *Neuron* **2**, 31-37.

Davies, J. A., Cook, G. M., Stern, C. D. and Keynes, R. J. (1990). Isolation from chick somites of a glycoprotein fraction that causes collapse of dorsal root ganglion growth cones. *Neuron* **2**, 11-20.

Dodd, J. and Schuchardt, A. (1995). Axon Guidance: a compelling case for repelling growth cones. *Cell* **81**, 471-474.

Durbin, R. M. (1987). Studies in the development and organization of the nervous system of *Caenorhabditis elegans*. Ph.D. Thesis, King's Colleges, Cambridge, England.

Forrester, W. C., Perens, E., Zallen, J. A. and Garriga, G. (1998). Identification of *Caenorhabditis elegans* genes required for neuronal differentiation and migration. *Genetics* **148**, 151-165.

Francis, R. and Waterston, R. H. (1991). Muscle cell attachment in *Caenorhabditis elegans*. *J. Cell Biol.* **114**, 465-479.

Frazier, D. T. and Narahashi, T. (1975). Tricaine (MS-222): effects on ionic conductances of squid axon membranes. *Eur. J. Pharmacol.* **33**, 313-317.

Goodman, C. S. (1996). Mechanisms and molecules that control growth cone guidance. *Ann. Rev. Neurosci.* **19**, 341-377.

Hallam, S. J. and Jin, Y. (1998). *lin-14* regulates the timing of synaptic remodelling in *Caenorhabditis elegans*. *Nature* **395**, 78-82.

Halloran, M. C. and Kalil, K. (1994). Dynamic behaviors of growth cones extending in the corpus callosum of living cortical brain slices observed with video microscopy. *J. Neurosci.* **14**, 2161-2177.

Harris, W. A., Holt, C. E. and Bonhoeffer, F. (1987). Retinal axons with and without their stomata, growing to and arborizing the tectum of *Xenopus* embryos: a time-lapse study of single fibres in vivo. *Development* **101**, 123-133.

Hatta, K. and Kimmel, C. B. (1993). Midline structures and central nervoys system coordinates in zebrafish. *Perspect. Dev. Neurobiol.* **1**, 257-268.

Hubener, M., Gotz, M., Klosterman, S. and Bolz, J. (1995). Guidance of thalamocortical axons by growth-promoting molecules in developing rate cerebral cortex. *Eur. J. Neurosci.* **7**, 1963-1972.

Keynes, R. J. and Cook, G. M. W. (1995). Repulsive and inhibitory signals. *Curr. Opin. Neurobiol.* **5**, 75-82.

Kirby, C., Kusch, M. and Kemphues, K. (1990). Mutations in the *par* genes of *Caenorhabditis elegans* affect cytoplasmic reorganization during the first cell cycle. *Dev. Biol.* **142**, 203-215.

Kolodkin, A. L. (1996). Growth cones and the cues that repel them. *Trends Neurosci.* **19**, 507-513.

Kolodkin, A. L., Matthes, D. J., O'Conner, T. P., Patel, N. H., Admon, A., Bentley, D. and Goodman, C. S. (1992). Fasciclin IV: sequence, expression, and function during growth cone guidance in the grasshopper embryo. *Neuron* **9**, 831-845.

Luo, Y. and Raper, J. A. (1994). Inhibitory factors controlling growth cone motility and guidance. *Curr. Opin. Neurobiol.* **4**, 648-654.

Matthes, D. J., Sink, H., Kolodkin, A. L. and Goodman, C. S. (1995). Semaphorin II can function as a selective inhibitor of specific synaptic arborizations. *Cell* **81**, 631-639.

McCarter, J., Bartlett, B., Dang, T. and Schedl, T. (1997). Soma-germ cell interactions in *Caenorhabditis elegans*: multiple events of hermaphrodite germline development require the somatic sheath and spermathecal lineages. *Dev. Biol.* **181**, 121-143.

McIntire, S. L., Reimer, R. J., Schuske, K., Edwards, R. H. and Jorgensen, E. M. (1997). Identification and characterization of the vesicular GABA transporter. *Nature* **389**, 870-876.

McMahon, A. P. (1993). Cell signalling in induction and anterior-posterior patterning of the vertebrate central nervous system. *Curr. Opin. Neurobiol.* **3**, 4-7.

Meima, L., Moran, P., Matthews, W. and Caras, I. (1997). Lerk2 (ephrin-B1) is a collapsing factor for a subset of cortical growth cones and acts by a mechanism different from AL-1 (ephrin-A5). *Mol. Cell Neurosci.* **9**, 314-328.

Myers, P. Z. and Bastiani, M. J. (1993). Growth cone dynamics during the migration of an identified commissural growth cone. *J. Neurosci.* **13**, 127-143.

O'Rourke, N. A. and Fraser, S. E. (1990). Dynamic changes in optic fiber terminal arbors lead to retinotectal map formation: an in vivo confocal microscope study. *Neuron* **5**, 159-171.

Orioli, D. and Klein, R. (1997). The eph receptor family: axonal guidance by contact repulsion. *Trends in Genetics* **13**, 354-359.

Raper, J. and Kapfhammer, J. (1990). The enrichment of a neuronal growth cone collapsing activity from embryonic chick brain. *Neuron* **4**, 21-29.

Shibata, A., Wright, M. V., David, S., McKerracher, L., Braun, P. E. and Kater, S. B. (1998). Unique responses of differentiating neuronal growth cones to inhibitory cues presented by oligodendrocytes. *J. Cell Biol.* **142**, 191-202.

Shoji, W., Yee, C. S. and Kuwada, J. Y. (1998). Zebrafish semphorin Z1a collapses specific growth cones and alters their pathway in vivo. *Development* **125**, 1275-1283.

Sretavan, D. W. and Reichardt, L. F. (1993). Time-lapse video analysis of retinal ganglion cell axon pathfinding at the mammalian optic chaism: growth cone guidance using intrinsic chiasm cues. *Neuron* **10**, 761-777.

Sulston, J. E. and Horvitz, H. R. (1977). Post-embryonic lineages of the nematode, *Caenorhabditis elegans*. *Dev. Biol.* **56**, 110-156.

Sulston, J. E., Schierenberg, E., White, J. G. and Thomson, J. N. (1983). The embryonic lineage of the nematode *Caenorhabditis elegans*. *Dev. Biol.* **100**, 64-119.

Taniguchi, M., Yuasa, S., Fujisawa, H., Naruse, I., Saga, S., Mishina, M. and Yagi, T. (1997). Disruption of semaphorin III/D gene cause severe abnormality in peripheral nerve projection. *Neuron* **19**, 519-530.

Tessier-Lavigne, M. and Goodman, C. S. (1996). The molecular biology of axon guidance. *Science* **274**, 1123-1133.

Thomas, C., DeVries, P., Hardin, J. and White, J. (1996). Four-dimensional imaging: computer visualization of 3D movements in living specimens. *Science* **273**, 603-607.

Walter, J., Kern-Veits, R., Huf, J., Stolze, B. and Bonhoeffer, F. (1987). Recognition of position-specific properties of tectal cell membranes by retinal axons in vitro. *Development* **101**, 685-696.

White, J. (1988). The anatomy. In *The Nematode Caenorhabditis elegans*, vol. I (ed. W. B. Wood), pp. 81-122. Cold Spring Harbor: Cold Spring Harbor Laboratory Press.

White, J. G., Southgate, E., Thomson, J. N. and Brenner, S. (1986). The structure of the nervous system of *Caenorhabditis elegans*. *Phil. Trans. Royal Soc. (Lond.)* B **314**, 1-340.

Yu, H.-H., Araj, H. H., Ralls, S. A. and Kolodkin, A. L. (1998). The transmembrane semaphorin sema I is required in *Drosophila* for embryonic motor and CNS axon guidance. *Neuron* **20**, 207-220.